A tyre wear modelling approach for vehicle dynamics simulation and control-oriented analyses with application to motorcycles

Stefano Radrizzani, Giulio Panzani and Sergio M. Savaresi

All the authors are with Dipartimento di Elettronica, Informazione e Bioingegneria, Politecnico di Milano, Via G. Ponzio 34/5, 20133, Milan, Italy

ARTICLE HISTORY
Compiled July 5, 2023

ABSTRACT
To increase vehicle dynamics modelling accuracy in simulation environments, in this work, we propose a model, where the mutual influence of the vehicle dynamics and tyre wear is taken into account. In this context, simulation-oriented models aim at representing the main features of the vehicle dynamics, while keeping the complexity low, making them suitable for control-oriented analyses and design. The wear model quantifies tyre wear as a tyre mass loss depending on the tyre-road interaction, derived from the vehicle dynamics and kinematics; then, the outcome of this model is consequently used to update the tyre friction characteristics, by modifying the main parameters of the Pacejka's magic formula. We also discuss the steps required to use the model in two-wheeled vehicles, where the roll dynamics plays an important role in the tyre wear. The main features of the developed model are discussed on a motorcycle, as a simulation case-study.

KEYWORDS
Tyre dynamics, Wear, Motorcycle, Simulation, Models

1. Introduction

The impact that tyres properties have on vehicle dynamics is a topic of unquestionable importance; for this reason, tyre modelling is a subject widely addressed in the scientific literature. Among the several topics of interest, one can find an understanding of the mechanisms that cause the degradation of tyre properties. As reported in [1], tyre degradation can be mainly related to two factors: the first one is the rubber abrasion induced by the tyre-road frictional interaction, when the tyre is actually rolling. The second cause is linked to the rubber oxidation caused by the interaction with the environment, and as such it could also arise when tyres are stored and left unused. This paper focuses on the first kind of phenomenon, in the following referred to as tyre wear, due to its tight two-way coupling with the vehicle dynamics, as will be detailed and clarified in the following.

Tyre wear modelling is a consolidated subject in the scientific literature, where the first relevant contributions date back to the mid-1900s. In most recent works, the characterization of the tyre wear is tackled by means of experimental correlations

Corresponding author: Stefano Radrizzani (stefano.radrizzani@polimi.it)

between tyre wear and tyre performance or also analytical models, with a different blending. Fully experimental and statistical correlations are proposed, for instance, in [2,3]. In [4–6], a tyre wear phenomenological correlation is coupled with an analytical lumped parameter brush model; in [7], a similar approach is applied to aeronautic tyres. Finally, finite element models are proposed in [8–11]. These works focus on the tyre wear modelling meant for evaluating the remaining tyre life or for tread wear predictions. Moreover, recent works have shown the potential benefits of taking into account tyre wear and vehicle dynamics interactions: for example, [12] presents the advantages of a calibration of an aircraft anti-skid controller aiming at reducing tyre wear, using a control-oriented tyre wear model.

Only a few works, to the best of the authors' knowledge, explicitly account for the tyre wear effects on the vehicle dynamics. In [13], test ring experiments are run on a broad selection of tyres in order to quantitatively assess the effect of tyre wear on the peak lateral force and overturning moment. A similar study is proposed in [14], where the focus is set on the longitudinal friction force and tyre mechanical stiffness, with respect to age and wear. Both works [13] and [14] show the impact of tyre wear on tyre forces, but they do not discuss how these consequences on tyre forces affect the tyre wear itself. Another approach is the one in [15] which proposes experimentally-based black-box correlations between some of the Pacejka's tyre parameters and tyre wear, temperature and inflating pressure; still, it lacks of a proper mechanism for the computation of such quantities (in particular, the tyre wear) and, as a matter of fact, the proposed model is only useful to adapt the tyre characteristic with respect to those parameters.

The above discussion shows that the literature lacks of an integrated modelling approach, where the vehicle dynamics affect the tyre wear and also, conversely, where the tyre wear is capable of affecting the vehicle dynamics – degrading the tyre capability of exerting forces. From a methodological perspective, the discussed works elaborate the vehicle data in an open-loop fashion, i.e., as input variables to their proposed tyre wear evaluation mechanism. In this way, the influence of vehicle dynamics and tyre forces on the tyre wear is solely addressed; the opposite interaction - i.e., how the tyre wear affects tyre forces and, as a consequence, the vehicle dynamics - is not considered.

The most complete approach to model the wear-tyre force interdependency is certainly presented in [16] where a detailed physical model of the tyre-road interaction accounts simultaneously for tyre temperature distribution, wear and resulting force capabilities. Despite the completeness of such an approach, this model is very complex, because it is based on finite elements. Recently, in [17], a simpler model to link tyre wear and tyre performance has been proposed. In particular, the sole tyre grip value was expressed as a function of the current tyre wear, quantified by an experimental look-up table. Then, the resulting grip value was introduced in a simplified vehicle model, used for the optimisation of a multi-lap strategy for racing cars.

In this work, we propose a simulation-oriented model, where the mutual influence of the vehicle dynamics and tyre wear is taken into account. Simulation-oriented models aim at keeping the model complexity low, but with sufficient accuracy to represent the main effects of a phenomenon; hence, they can be also used in a control-oriented perspective. Toward this aim, the model should be able to compute the mutual relationship between tyre wear and tyre forces to be easily integrated into vehicle simulators, which could also be run in real-time, i.e., for driving simulators or video-games. These features are the reason why the model is also suitable for control-oriented purposes, i.e., when the model is used to formulate and tune control strategies. For example, in

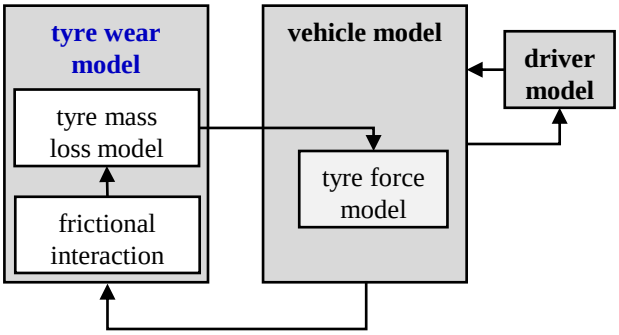

Figure 1.: Block-diagram of the interaction between the developed tyre wear model and the vehicle dynamics model.

this case, to control the tyre wear in real-time [12] or optimize the strategy in racing scenarios [17]. As a consequence, complex models, like [16], are not suitable for simulation/control objectives.

The approach we propose quantifies tyre wear as a tyre mass loss depending on the tyre-road interaction, derived from the vehicle dynamics and kinematics. Then, the outcome of this model is consequently used to update the tyre friction characteristics; in particular, the friction peak and the cornering stiffness of the tyre. In this way, the followed approach merges the gap between the models for the tyre wear evaluation and the tyre forces model, integrating these two kinds of model. In particular, in order to keep the model complexity low – required by the control and dynamic simulation purposes – the wear model is based on first-principle and classic experimental correlations, and its influence on the vehicle dynamics is achieved by suitably adapting the Pacejka's tyre model parameters: this solution allows for a simple integration of the proposed model into existing multi-body vehicle dynamics simulators, which typically rely on the Pacejka's model to describe the tyre. A graphical block-diagram of the model interactions is shown in Figure 1.

The proposed approach is initially developed for a classic four-wheeled vehicle. Then, it is also extended to the dynamics of two-wheeled vehicles. As a matter of fact, the role of the vehicle roll angle – which is a distinguishing feature of two-wheelers – has to be explicitly taken into account in the tyre wear model. Indeed, the roll dynamics not only is highly significant in motorcycles but also generates non-uniform wear on the tyre, e.g., wear could differ between the right and left shoulder of the tyre.

Finally, in order to highlight the features of the tyre wear model, the proposed approach is integrated into a commercial motorcycle simulator, and a simulation case study is discussed.

The main contribution of our work are: 1) the integration of classical models for tyre wear and tyre forces, to simulate the mutual influence between wear and forces in tyres; 2) the extension of wear models to motorcycles, also considering a different level of tyre wear, and so performance, depending on the contact region of the tyre.

The paper is organized as follows: in Section 2, a first-principle tyre wear model, based on scientific literature suggestions, is recalled and described. Then, the effects

of tyre wear on frictional forces are discussed in Section 3. In Section 4, the model is tweaked so as to suit motorcycle tyres and eventually tested in a simulation environment in Section 5.

2. Tyre wear model

Wear is defined, see [8], as the material removal from a surface – in this case, the tyre one – subject to a frictional interaction with another surface – the road – and it arises when they are sliding with respect to each other. This definition highlights the two main aspects to be considered in the development of a tyre wear model: 1) the description of the *frictional interaction* between the tyre and the road; 2) the quantification of the amount of tyre wear, eventually related to the *tyre mass loss*.

In the following, after discussing the several possibilities disclosed in the scientific literature, we present the one employed in this work. It will also serve as the basis to understand the modifications proposed to handle the two-wheeled case.

2.1. Computation of the frictional interaction

There is a common agreement within the scientific literature that tyre wear is mostly correlated to the frictional energy dissipated in the tyre-road interaction. Indeed, a typical approach to model tyre wear is based on the computation of the frictional power, which is then explicitly taken into account in the tyre wear model, e.g., [4,5,7, 9,11]. The main difference among the mentioned approaches lies in the level of details used to model and then compute the frictional power and the corresponding tyre wear. Microscopic – based on Finite Elements Methods (FEM) – and lumped parameters models approach the frictional power computation from a local perspective, modelling the tyre as a set of dynamic elements interacting among themselves and with the road; the frictional power is the result of each local interaction, integrated over the overall tyre. Finite elements are particularly preferred for detailed analysis: to mention a few examples, in [11], the wear distribution across the tyre profile is computed and in [9] the focus is set on comparing different complicated tread patterns in terms of tyre wear. Lumped parameter models – see e.g., [4,5,7] – aim at similar goals but are more suitable for experimental validations and analyses, as the parameters of the lumped models are easier to be identified.

In a control-oriented vehicle dynamics perspective, the use of the discussed models is unnecessary, as they provide a level of detail which is not controllable with the available vehicle dynamics actuators, operating at a macroscopic level. In addition, even for simple simulation-oriented purposes the complexity of these models, typically FEM ones [18], could be detrimental. In vehicle dynamics applications, the local tyre-road frictional interactions are commonly summarized at a macroscopic scale, describing the longitudinal F_x and lateral F_y tyre forces as functions of the wheel longitudinal λ and lateral α slip. These quantities, firstly introduced from the analysis of a simple tyre brush model, summarize the local tyre compliance and its relative motion with respect to the road, using two macroscopic variables that can be easily calculated from the tyre kinematics, when considered as a whole rigid body [19]. Indeed, the longitudinal and lateral slip are computed as follows:

$$\lambda = \frac{v_x - R_{\mathrm{w}}\omega}{v_x} \text{ and } \alpha = \operatorname{atan}\left(\frac{v_y}{v_x}\right), \tag{1}$$

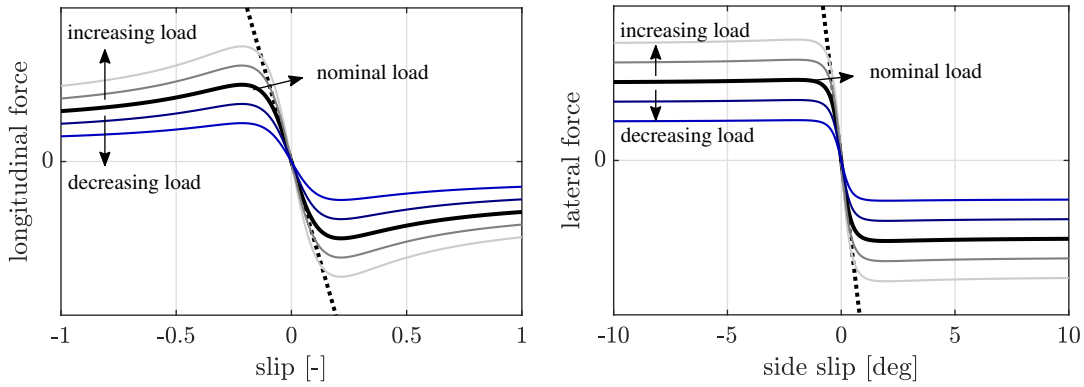

(a) Longitudinal force.

(b) Lateral force.

Figure 2.: A qualitative example of the tyre friction forces. The effects of vertical load variation are highlighted for increasing and decreasing loads.

where v_x and v_y are the longitudinal and lateral components of the vehicle linear speed v; R_w is the wheel radius and ω is the angular wheel speed. A suitable model for the frictional forces is given by the Pacejka's *magic formula* (MF) [19], which is an empirical parametric model able to describe the static and dynamic properties of tyre forces [20]. The simplest version of the Pacejka's equations is given by the following equations:

$$F_x = \mu_\lambda F_z \sin(c_\lambda \mathrm{atan}(b_\lambda \lambda)) \text{ and } F_y = \mu_\alpha F_z \sin(c_\alpha \mathrm{atan}(b_\alpha \alpha)), \tag{2}$$

where F_z is the vertical load and μ, c, b are experimental coefficients, possibly function of multiple factors. A qualitative example of a Pacejka's tyre force model is depicted in Figure 2, it shows the longitudinal and lateral forces as functions of sliding speed and how they are linked with the vertical load, that acts as a scaling factor as a first approximation. The two principal parameters that describe such curves are the cornering stiffness (C_λ and C_α), that is the slope of the force curve in the linear region around the origin, and the maximum force values, usually normalized with respect to the actual load (μ_λ and μ_α).

Starting from the only longitudinal dynamics of a *single corner model* (Figure 3a), the longitudinal force balance and the torque balance at the wheel are

$$\begin{cases} M_\mathrm{v}\dot{v} &= F_x \\ J_\mathrm{w}\dot{\omega} &= -F_x R_\mathrm{w} + T_\mathrm{mot} - T_\mathrm{brake} \end{cases}, \tag{3}$$

where M_v is the single corner vehicle mass, J_w the wheel inertia and T_mot, T_brake are the traction and braking torque at the wheel respectively. From (3), it is possible to obtain the total power balance in (4) by summing the two equations, multiplied for v and ω respectively:

$$\underbrace{M_\mathrm{v}\dot{v}v + J_\mathrm{w}\dot{\omega}\omega}_{\substack{\text{power related to} \\ \text{kinetic energy}}} = \underbrace{F_x\left(v - R_\mathrm{w}\omega\right)}_{\textbf{frictional power}} + \underbrace{T_\mathrm{mot}\omega - T_\mathrm{brake}\omega}_{\substack{\text{motor/brake} \\ \text{power}}}. \tag{4}$$

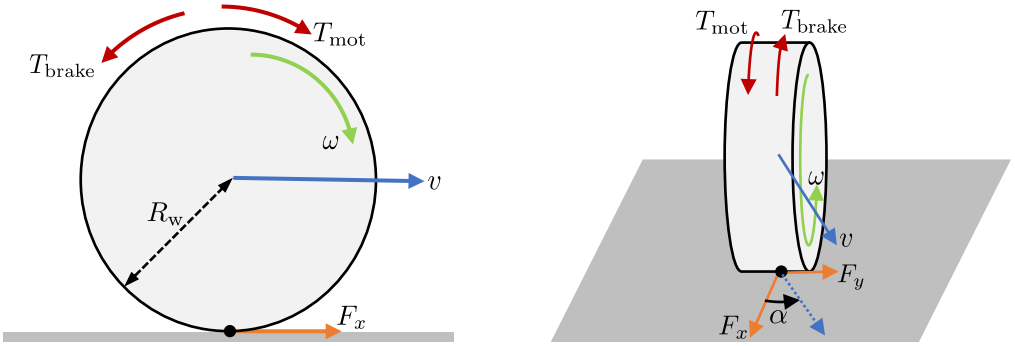

(a) Longitudinal wheel dynamics.

(b) Longitudinal and lateral dynamics.

Figure 3.: Graphical description of the variables involved in longitudinal and lateral tyre dynamics.

Highlighting the easily recognizable terms related to kinetic energy and motor or brake power, the frictional power in the longitudinal case can be written as:

$$W = F_x \underbrace{(v - R_{\text{w}}\omega)}_{\substack{\text{sliding} \\ \text{speed}}} = F_x v \lambda, \tag{5}$$

where $v - R_{\text{w}}\omega$ represents the longitudinal sliding speed of the wheel contact point. From (5), two considerations can be done: 1) the frictional power is always negative, because F_x and λ have always the opposite sign (Figure 2a); 2) the dissipated power increases with λ: therefore, as common experience suggests, wheel locking or skidding are situations of extreme tyre wear

Moreover, considering the linear region of the longitudinal forces, the frictional power computation becomes easier, resulting in a proportional relationship to the vehicle speed and with the slip squared:

$$W = C_\lambda v \lambda^2. \tag{6}$$

The computation of the frictional power can be generalized to the scalar product between the frictional force and the sliding velocity of the contact point. Therefore, when also the lateral dynamics is considered (Figure 3b) the following equation [5,6] holds:

$$W = F_x v_{x,\text{sliding}} + F_y v_{y,\text{sliding}} = F_x \underbrace{(v\cos\alpha - R_{\text{w}}\omega)}_{\substack{\text{longitudinal} \\ \text{sliding} \\ \text{speed}}} + F_y \underbrace{v \sin\alpha}_{\substack{\text{lateral} \\ \text{sliding} \\ \text{speed}}}. \tag{7}$$

Also for the longitudinal and lateral vehicle dynamics, linearising (7), the friction power grows proportionally to vehicle speed and the square of the longitudinal and

side slip:

$$W = C_\lambda v \lambda^2 + C_\alpha v \alpha^2. \tag{8}$$

In conclusion, in a vehicle dynamics oriented simulation, (7) provides a simple, yet effective, way to compute the frictional power.

2.2. Computation of the tyre mass loss

In order to quantify the tyre wear, the tyre mass loss is a suitable quantity. As already discussed when presenting tyre force models, for our purposes, detailed finite elements approaches for the tyre mass loss induced by wear – see e.g., [9–11] – are oversized. In order to characterize the wear in a simpler way, we introduce the experimental law in [8], that directly links the mass loss rate with the frictional power. In the case of tyres, the contact with the ground is not localized in a single point, but it is distributed over an area, therefore the mass loss rate and the frictional power are usually normalized with respect to the contact area a_c [2] and they are related by an experimental function $\mathcal{M}$:

$$\frac{\mathrm{d}m}{\mathrm{d}t} = \mathcal{M}(W) = K_1 \left(\frac{|W|}{a_\mathrm{c}} \right)^{K_2}, \tag{9}$$

where $m = \frac{M_\mathrm{loss}}{a_\mathrm{c}}$ is the mass loss M_loss per contact area a_c and K_1, K_2 are two positive model parameters, characteristic of the considered tyre. From (9), the time evolution of the overall tyre mass loss is:

$$M_\mathrm{loss}(t) = \int_{t_0}^{t} a_\mathrm{c} \mathcal{M}(W) \mathrm{d}t. \tag{10}$$

2.3. Discussion on tyre wear model features

The tyre wear model can be derived combining equations (7) and (10):

$$\begin{cases} W = F_x \left(v \cos\alpha - R_\mathrm{w} \omega \right) + F_y v \sin\alpha \\ M_\mathrm{loss}(t) = \int_{t_0}^{t} a_\mathrm{c} \mathcal{M}(W) \mathrm{d}t \end{cases}. \tag{11}$$

The considered model (11) relates the tyre wear to its first-order impact sources [21]: the sliding speed and the vertical load, as visible in the Pacejka's MF in (2) and in Figure 2. It is well-known, see [21], that other factors impact the tyre wear; among the several, one can mention the tread core temperature, the tyre inflation pressure, the rubber viscoelasticity, the tyre geometry and road specific properties, like its roughness. The presented modelling approach assumes that all the mentioned factors contribute to the tyre wear through the definition of the Pacejka's *magic formula* parameters and the parameters K_1 and K_2, appearing in (9).

Nonetheless, specific influences can be accounted for in the employed tyre wear model. In the following, we present possible modifications of (11), which are able to include the effect of these variables. We categorize these modifications as direct and indirect: the former refers to mechanisms that have an immediate impact on the mass loss computation (10); the latter refers to changes in the tyre force relationships, which

eventually have an impact in the frictional power quantification (7). In both cases, as will be clear in the following, explicit correlations must be available, either based on analytical or empirical evidence. Given that these correlations are available for the tread core temperature T and tyre inflation pressure P, these two will be addressed in the following. However, to further improve the model, the presented rationale can be applied to other effects.

2.3.1. Second-order indirect effects

Tyre forces are influenced by different variables [22]; among them, pressure and temperature play an important role. They can be explicitly included as additional inputs of the tyre wear model, so that (7) becomes:

$$W = W(T,P) = F_x(T,P)\left(v\cos\alpha - R_{\mathrm{w}}\omega\right) + F_y(T,P)v\sin\alpha. \tag{12}$$

Commonly, e.g., [23], the normalized displacement with respect to the reference value ξ_0:

$$\delta\xi = \frac{\xi - \xi_0}{\xi_0},\ \xi = \{T,P\}, \tag{13}$$

is used as input of polynomial scaling factors of MF parameters Ξ:

$$\Xi = \Xi_0\left(1 + \theta_{\xi,1}\delta\xi + \theta_{\xi,2}\delta\xi^2 + ...\right), \tag{14}$$

so that, when the variable ξ is equal to the reference one ξ_0, the parameter Ξ coincides with the reference value Ξ_0.

In the case of pressure, coefficients θ_P can be fitted on the main parameters of the Pacejka's *magic formula*: the cornering stiffness and the friction peak [24,25] using data obtained at the disk ring for different levels of pressure. Similar correlations are available in [26] when road roughness is concerned. To include the effect of the tyre surface temperature on friction curves, the variation of the Pacejka's parameters can be studied as well, see [27]. In real-time simulation environments, moreover, a tyre thermal model (see e.g., [17,28,29]) is frequently employed, to account for temperature variations during the operation of the tyre.

2.3.2. Second-order direct effects

The direct effect of pressure in the mass loss rate in (9) is visible in how it influences the shape of the contact area [25]:

$$a_{\mathrm{c}} = a_{\mathrm{c}}(P), \tag{15}$$

that increases at lower pressure levels. A correlation, based on experimental laws, between the tyre pressure and the contact area has been already introduced in more recent and improved versions of the Pacejka's MF [24].

Temperature affects the chemical properties of the tyre during the abrasion process, increasing the mass loss rate [21], therefore an additional temperature-dependant pa-

rameter can be introduced in (9):

$$\mathcal{M}(W,T) = K_1 K_{\mathrm{t}}^{T-T_0} \left(\frac{|W|}{a_c}\right)^{K_2}, \tag{16}$$

where T_0 is the reference temperature used to define K_1 and K_{t} is a positive parameter grater than one.

Additional tyre wear is generated if the tyre is overstressed, and so typically in racing vehicles, when the temperature differs from the nominal one. This phenomenon – known as graining, at cold temperatures, and blistering, at hot temperatures – can be also included in the mass rate computation [17,29]:

$$\begin{aligned} \mathcal{M}(W,T) \;\; = \;\; & K_1 K_{\mathrm{t}}^{T-T_0} \left(\tfrac{|W|}{a_c}\right)^{K_2} + K_{\mathrm{g},1} \max(T_{\mathrm{t}} - T, 0))^{K_{\mathrm{g},2}} + \\ & + K_{\mathrm{b},1} \max(T - T_{\mathrm{t}}, 0))^{K_{\mathrm{b},2}}, \end{aligned} \tag{17}$$

where T_{t} is the transition temperature between graining and blistering, and K_{g} and K_{b} are positive parameters, related to graining and blistering wear, respectively.

2.4. Tyre thermal model

In the proposed tyre wear model, temperature affects the tyre wear model in two ways. First of all, it modifies the tyre contact forces, given that Pacejka's model is written as a function of the temperature, as shown in (12). Then, temperature changes also the properties of tyres; therefore, the tyre wear rate is a direct function of the temperature, as visible in (16) and (17).

However, to consider the tyre temperature variability while driving the vehicle, a subsequent thermal model is necessary. In the current literature, similarly to tyre wear models, thermal models range from lumped models, to complex distributed ones based on finite elements, some examples of the two approaches are in [16,17,28–30]. To maintain the same paradigm of the tyre wear framework discussed in this paper, we propose to use a simpler version of the lumped model shown in [17,29]:

$$\frac{\mathrm{d}T}{\mathrm{d}t} = \alpha_0 W - \alpha_{\mathrm{amb}}(T - T_{\mathrm{amb}}) - \alpha_{\mathrm{road}}(T - T_{\mathrm{road}}), \tag{18}$$

where T_{amb} and T_{road} are the ambient and road temperature, respectively; and they can be considered input signals of the model. Then, α_0, α_{amb} and α_{road} are model parameters.

Referring to (18), it is interesting to see the mutual influence between the tyre frictional power and the temperature itself, given that a portion of the frictional power is dissipated through an increase in the tyre temperature. Finally, higher accuracy and complexity thermal models can be derived by finding experimental correlations between the thermal parameters and tyre wear itself. Indeed, as mentioned in [16], the thermal inertia of the tyre reduces when tyre mass and tread are consumed due to wear itself.

3. Tyre wear effects on friction forces

Tyre wear arises as a loss of tyre performance, visible as a degradation of the tyre capability of exerting forces and, it can be practically quantified as a reduction of cornering stiffness and force peak in longitudinal and lateral forces. This implies that on worn tyres: 1) the maximum transmittable force is lower; 2) to generate forces, a higher longitudinal slip or sideslip has to be reached, with respect to the same tyre when new. These aspects are discussed in [15] or [16], and experimentally verified on a SUV in [14]. The consequences of tyre wear are also experienced in everyday situations. They are clearly visible in racing scenarios, where lap-time performance reduces on worn tires [17]; and also in common driving, when braking phases become longer and possibly unsafe when tyres are worn [31].

In this section, an experimental approach to link tyre wear and this loss of performance in the tyre forces is discussed. Following the same rationale used to make the MF parameters dependent on some additional variables, as in (14), first of all, a tyre wear index is defined, then it is used to update the main parameters of the friction forces, correlating tyre wear and tyre characteristics.

3.1. Tyre wear index definition

The tyre wear model can be summarized defining a tyre wear index. Typically, it is defined as the ratio between the current tread thickness and the nominal one, e.g., [14,17]. However, to have a direct correlation between the tyre index and the tyre wear model, we employed an index I_m, defined as the ratio between the current tyre mass and the original one when new M_0:

$$I_m(t) = \frac{M_0 - M_{\text{loss}}(t)}{M_0}. \tag{19}$$

Indeed, M_{loss} is a function of $\mathcal{M}$. To implement the model in a simulation environment, the tyre wear index evolution is computed turning (19) into its discrete-time form:

$$I_m(t) = I_m(t-1) - \tau \frac{\mathcal{M}(t)}{M_0}, \tag{20}$$

where τ is the sampling time of the simulation.

This index has two important properties: 1) it is a non-dimensional number that represents the percentage of current tyre mass with respect to the original one; 2) it always decreases in time, given that the mass loss rate (9) is always positive.

3.2. Tyre wear index and tyre forces relationship

Applying the same rationale of (14), the tyre wear index has the same structure of $\delta\xi$ variables, defined in (13), and so it can be used to scale the parameters of the Pacejka's *magic formula*. In particular, the main ones affected by tyre wear: the maximum grip

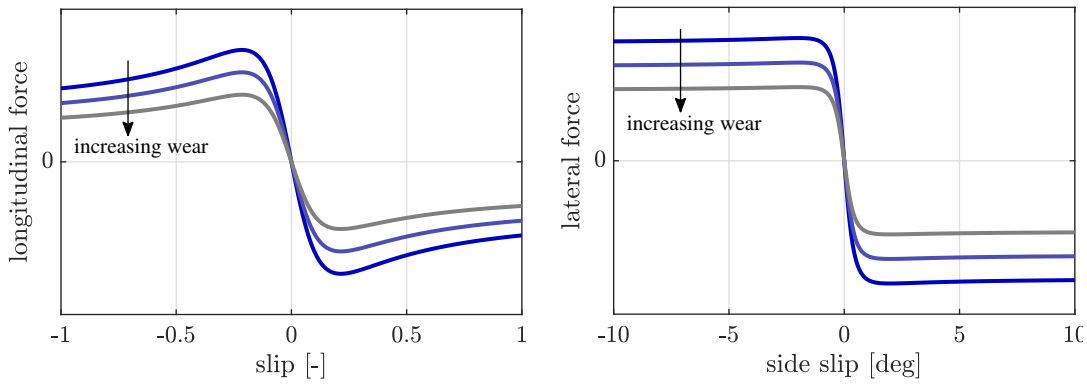

(a) Longitudinal force.

(b) Lateral force.

Figure 4.: A qualitative example of the tyre friction forces evolution as functions of the wear level.

and the cornering stiffness, [5,16]. Therefore, the following equations are introduced:

$$\begin{array}{rcl} C_\lambda & = & C_\lambda^0 \cdot \left(1 + \theta_{C\lambda,1}\delta I_m + \theta_{C\lambda,2}\delta I_m^2 + ...\right) \\ \mu_\lambda & = & \mu_\lambda^0 \cdot \left(1 + \theta_{\mu\lambda,1}\delta I_m + \theta_{\mu\lambda,2}\delta I_m^2 + ...\right) \\ C_\alpha & = & C_\alpha^0 \cdot \left(1 + \theta_{C\alpha,1}\delta I_m + \theta_{C\alpha,2}\delta I_m^2 + ...\right) \\ \mu_\alpha & = & \mu_\alpha^0 \cdot \left(1 + \theta_{\mu\alpha,1}\delta I_m + \theta_{\mu\alpha,2}\delta I_m^2 + ...\right) \end{array}, \tag{21}$$

where the superscript 0 refers to the parameter value when the tyre is new and θ is the set of parameters.
If possible, the parameters θ could be found with some fitting procedure on experimental data collected during different levels of wear. Given that these data are typically hard to obtain, (21) can be simplified by introducing a heuristic link between I_m and the forces, derived from the experimental data collected in [14]:

$$\begin{array}{rcl} C_\lambda & = & C_\lambda^0 \cdot I_m \\ \mu_\lambda & = & \mu_\lambda^0 \cdot I_m \\ C_\alpha & = & C_\alpha^0 \cdot I_m \\ \mu_\alpha & = & \mu_\alpha^0 \cdot I_m \end{array}. \tag{22}$$

The effects of this model on the friction model are shown in Figure 4, while more general consequences on the vehicle dynamics are discussed in the case study in Section 5.

4. Tyre wear model for motorcycles

The tyre wear model discussed in the previous sections cannot be immediately used in two-wheeled vehicles, mainly due to the significant differences in the roll dynamics and the related tyre forces. Indeed, car tyres are subject to a small and constant camber angle, named γ in Figure 5, defined as the angle between the tyre vertical axis and the axis normal to the ground. On the other hand, in motorcycles, the camber angle varies widely over time when the motorcycle is rolling – so that it is also called roll angle –

reaching up to 60 deg, in particular in racing ones. As consequence on the tyre wear model, significant and varying camber angles not only affect the tyre forces generation mechanism but also the portion of tyre patch that is in contact with the ground.

In the following of the section, it will be shown how to deal with these two aspects in the previously proposed model.

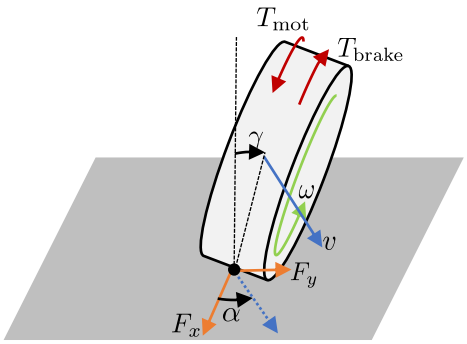

Figure 5.: Graphical description of the variables involved in the lateral wheel dynamics in rolling conditions.

4.1. Longitudinal and lateral slip

In the presence of a camber angle, the definition of longitudinal and lateral slip should consider some specific aspects [32,33]. First of all, the camber angle makes the sliding speed of the contact point differs from the one at the centre of the wheel. Therefore, in the slip computation in (1), v_x and v_y refer to speeds at the contact point of the wheel. Secondly, the computation of the longitudinal slip λ, and so of the frictional power, is corrected by considering the equivalent radius of the tyre. Assuming that the tyre has a circular profile with radius R_{tyre}, it can be computed as:

$$R_{\text{w,eq}} = R_{\text{w}} - R_{\text{tyre}}(1 - \cos\gamma). \tag{23}$$

4.2. Lateral force generation mechanism

High camber angles in motorcycle tyres make a deeper analysis of the force mechanism generation in tyres necessary. Indeed, when the camber angle is null, the force component induced by the elasticity of the tyre is mainly vertical, having a small impact on lateral and longitudinal tyre forces. On the other hand, when a motorcycle is rolling, the elastic force impacts the lateral force component [34,35], which can be seen as the sum of two different contributions [25,33]: the frictional one generated when the tyre is sliding $F_{y,\alpha}$ and the elastic one $F_{y,\gamma}$:

$$F_y = F_y(\alpha,\gamma) \quad = \quad \underbrace{F_{y,\alpha}}_{\textbf{frictional force}} \quad + \quad \underbrace{F_{y,\gamma}}_{\text{elastic force}} . \tag{24}$$

When considering small side slip angles, the model in (24) can be linearised:

$$F_y = C_\alpha \alpha + C_\gamma \gamma, \tag{25}$$

where C_γ is the camber stiffness. The linear model is particularly useful to show an important property of (24): in motorcycles, lateral forces can be generated by increasing the slip value or, alternatively, by increasing rolling [36].

To model this kind of phenomena in the tyre forces generation, the Pacejka's *magic formula* has been modified, as shown in [32], exploiting the two forces contributions, becoming more accurate for two-wheeled vehicles. The shape of the lateral forces is qualitatively reported in Figure 6.

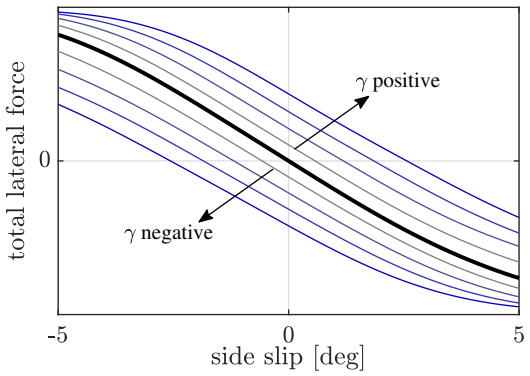

Figure 6.: Total lateral force function of side slip angle at different camber angles, highlighting the characteristic at zero camber angle, that is the one passing through the origin of the axis.

Finally, as a consequence in the tyre wear model, it should be taken into account that the force generated by camber $F_{y,\gamma}$ is an elastic force. It follows that the computation of the frictional power in (7) is extended to have the lateral power contribution as a function of the sole lateral forces generated by friction $F_{y,\alpha}$:

$$W = F_x \left(v \cos\alpha - R_{\mathrm{w,eq}}\omega\right) + F_{y,\alpha} v \sin\alpha. \tag{26}$$

It can be noticed that (26) is equivalent to (7) when the motorcycle is not rolling; indeed, $F_{y,\alpha} = F_y$ and $R_{w,eq} = R_{\mathrm{w}}$ when $\gamma = 0$.

4.3. Tyre wear index for motorcycles

Considering that, when a motorcycle is rolling, the contact area laterally slides on the tyre profile. the wear could be differently distributed on the tyre. In general, three main zones of wearing arise: the central region, and the right and left shoulders, as shown in Figure 7.

It follows that a single tyre wear index, as (19), has an insufficient level of modelling detail, because it assumes a uniform wear on the tyre. Therefore, three independent tyre wear indexes are constructed, evolving only when the contact area is actually in

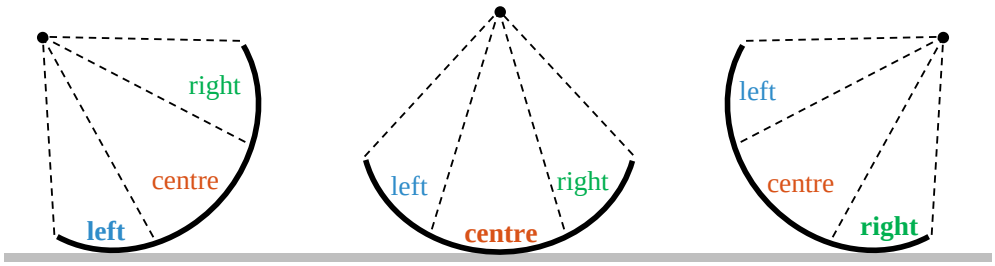

Figure 7.: Three main zones of wearing in motorcycle tyres.

one's region:

$$\begin{array}{lcll} I_{m,\text{left}}(t) & = & I_{m,\text{left}}(t-1) & - \quad \sigma_{\text{left}}(\gamma)\tau\frac{\mathcal{M}(t)}{M_0} \\ I_{m,\text{centre}}(t) & = & I_{m,\text{centre}}(t-1) & - \quad \sigma_{\text{centre}}(\gamma)\tau\frac{\mathcal{M}(t)}{M_0} \\ I_{m,\text{right}}(t) & = & I_{m,\text{right}}(t-1) & - \quad \sigma_{\text{right}}(\gamma)\tau\frac{\mathcal{M}(t)}{M_0} \end{array} , \tag{27}$$

where σ are boolean variables defined as follows:

$$\begin{array}{lcl} \sigma_{\text{left}} = 1 & \Leftrightarrow & \gamma \in \left[-\gamma_{\max}, -\frac{1}{3}\gamma_{\max}\right] \\ \sigma_{\text{centre}} = 1 & \Leftrightarrow & \gamma \in \left[-\frac{1}{3}\gamma_{\max}, \frac{1}{3}\gamma_{\max}\right] \\ \sigma_{\text{right}} = 1 & \Leftrightarrow & \gamma \in \left[\frac{1}{3}\gamma_{\max}, \gamma_{\max}\right] \end{array} . \tag{28}$$

The parameter $\gamma_{\max}$ can be chosen in order to exploit the maximum range of camber angles reached. For example, in racing riding styles, the rider rolls up to 60 deg; while for standard riders, 45 deg of camber angle are usually reached.

Finally, a continuous index $I_m(\gamma, t)$ with respect to the roll angle is defined by linearly interpolating the centre of the three regions previously discussed. A graphical interpretation is in Figure 8.

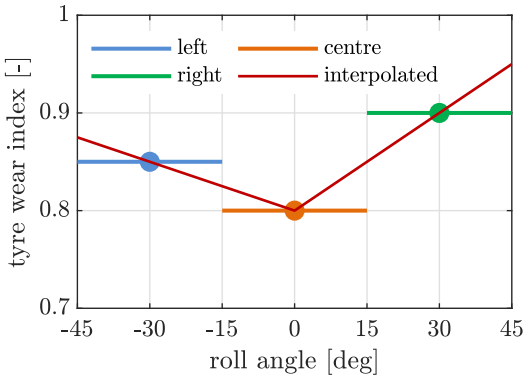

Figure 8.: Interpolated tyre wear index function of roll angle at a fixed time instant.

To increase the model accuracy, this approach is generalized to an arbitrary number

of sectors N_{sect}. In this case, the detection of the active sectors needs to be deeper analysed, because the number of active sectors N_{a} depends on how many sectors are simultaneously in contact with the ground. Hence, the activation function of the *i-th* sector σ_i depends not only on the camber angle γ, but also on the width w_{c} of tyre contact area, as graphically depicted in Figure 9.

The tyre contact area width is computed in the Pacejka's *magic formula* framework, as discussed in [24], and possibly even pressure-variant.

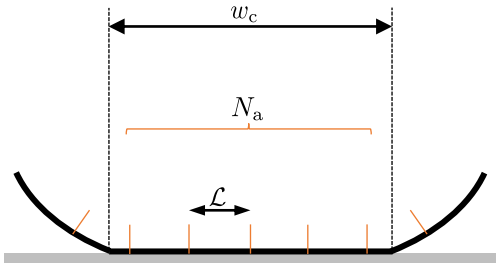

Figure 9.: Graphical interpretation of the number of active set computation.

It follows that the tyre wear index of the *i-th* sector is defined as:

$$I_{m,i}(t) = I_{m,i}(t-1) - \sigma_i(\gamma, w_{\text{c}})\tau\frac{\mathcal{M}(t)}{M_0},\ i = 1, ..., N_{\text{sect}}. \tag{29}$$

To compute $\sigma_i(\gamma, w_{\text{c}})$, the knowledge of which sectors are active is necessary. The first step is the computation of N_{a}, that – according to Figure 9 – is the ceil approximation of the ratio between w_{c} the length of tyre profile per sector $\mathcal{L}$:

$$N_{\text{a}}(w_{\text{c}}) = \left\lceil \frac{w_{\text{c}}}{\mathcal{L}} \right\rceil. \tag{30}$$

$\mathcal{L}$ can be found using the circular approximation of the tyre:

$$\mathcal{L} = R_{\text{tyre}}\gamma_{\text{sect}} = R_{\text{tyre}}\frac{2\gamma_{\max}}{N_{\text{sect}}}. \tag{31}$$

Once having found the number of active sectors, the range of active sectors is composed by the N_{a} sectors centred in the current camber angle γ. It follows that, the activation function of the *i-th* sector σ_i is defined as:

$$\sigma_i(\gamma, w_{\text{c}}) = 1 \Leftrightarrow \gamma - \frac{N_{\text{a}}}{2}\gamma_{\text{sect}} \leq -\gamma_{\max} + \left(i - \frac{1}{2}\right)\gamma_{\text{sect}} \leq \gamma + \frac{N_{\text{a}}}{2}\gamma_{\text{sect}}. \tag{32}$$

5. Tyre wear model features: A simulation case study

In order to highlight the features of the proposed tyre wear model, it has been implemented in MotorcycleMaker[1], a commercial multi-body simulator for motorcycle

[1]MotorcycleMaker, IPG Automotive, Karlsruhe, Germany.

dynamics and rider behaviour, interacting with Simulink[2] environment. The considered motorcycle is a default Honda-CBR600 and the main Pacejka's *magic formula* parameters are listed in Table 1. Finally, inflation pressure and temperature are set constant to the nominal value.

Table 1.: Tyre Nominal Parameters

	Rear	**Front**	
model	180/55/R17	120/70/R17	
μ_λ^0	1.279	1.122	-
C_λ^0	127.34	85.68	kN
μ_α^0	1.17	1.104	-
C_α^0	469.5	460.46	N/deg
C_γ^0	15.31	25.49	N/deg
M_0	6.2	4.1	Kg

The simulations will take place at the Hockenheimring short track, where a single lap is 2.4 km long and characterized by a higher number of right turns.

The tyre wear model properties are discussed performing different sensitivity analyses, in particular, neglecting the thermal tyre dynamics, the tyre wear evolution is analysed as a function of: 1) the tyre parameters K_1 and K_2; 2) the riding style; 3) the number of sectors N_{sect}.

5.1. Sensitivity w.r.t. the tyre wear parameters

This section aims at presenting the evolution of the tyre wear index, varying the parameters K_1 and K_2, in order to show the effects on the vehicle dynamics that the wear implies. In this analysis, the number of sectors is 3 and they are related to the centre and the two tyre shoulders. In Figure 10, the behaviour of the rear centre index for four different couples of values is shown. It is clear that wear increases with higher values; in particular, it is more sensible to the value K_2, because it acts in an exponential way on the rate, as shown in (9). Therefore, the model can easily represent a wide range of tyres, just shaping the two parameters: low values can model the behaviour of standard tyres whose nominal life is in the order of hundreds of thousand kilometres; high values are able to model sport tyres that run out after a low number of circuit laps.

Considering the highest wear rate case ($K_1 = 200\text{e-}10$ and $K_1 = 1.5$), the capability of modelling different levels of wear on each tyre sector is shown in Figure 11. In particular, it is visible that wear results to be higher in the central portion of the tyre. Indeed, traction and braking phases occur at small roll angles, where the frictional power is higher, because of the increasing of tyre longitudinal forces and slip. Then, wear is much higher on the right side than the left one, in fact, the considered circuit is characterized by a higher number of right turns.

The consequences of tyre wear on the vehicle dynamics are visible in Figure 12. It shows the loss of performance of the tyre due to wear: in particular, it is visible that the same force is returned with a higher slip value when the tyres are worn. Coherently with the tyre wear indexes in Figure 11, the highest effects of wear are visible on the front tyre, particularly in the longitudinal force on the front, indeed braking phases

[2]Simulink, Mathworks, Natick, MA, USA.

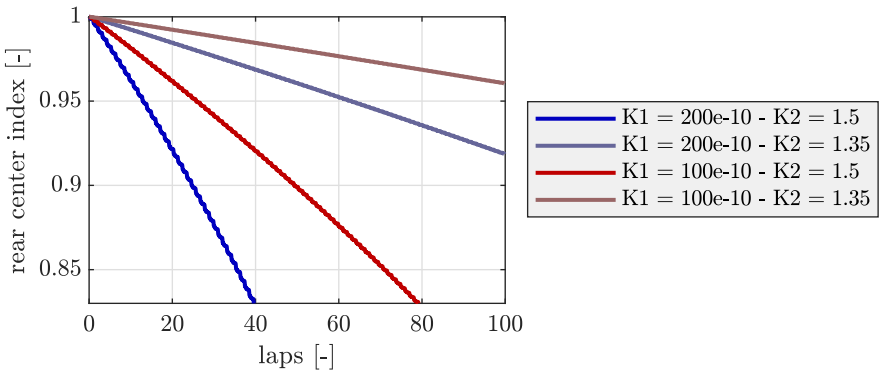

Figure 10.: Sensitivity analysis with respect to parameters K_1 and K_2, resulting in a faster wearing for higher parameters values.

occurring at small roll angles, are associated with the highest wear index sector (the front centre one).

5.2. Sensitivity w.r.t. the riding style

Riding style has a significant impact on tyre wear [37], indeed the more aggressive the driving style is, the more demanding the tyre forces and slips request is. To verify the capability of the model to show this, two different riding styles are considered; in particular, a normal and a cautious rider are compared. To model the riding style, different limits on the *gg-plot* (see e.g., [38,39]) are imposed in the simulation environment, as visible in Figure 13b. In Figure 13a, the wear indexes evolution for two different styles are reported, showing a slower evolution for the indexes associated with a more cautious riding style, as expected.

5.3. Sensitivity w.r.t. the number of sectors

In this last sensitivity analysis, the possible advantages of using a higher number of sectors are discussed. To this aim, the focus is given on the tyre wear index profile, that is the value assumed by the index for each roll angle. In particular, the 3-sector model is compared with a 27-sector one. Figure 14a show the coherence between the two, highlighting the capability of better reproducing wear shapes when the sectors increase.

Recalling the expression in (30), the contact patch width plays an important role in the model with more than 3 sectors. Therefore, two additional simulations have been run, modifying the default MF parameters in order to have a wider and narrow contact area, typically derived from incorrect pressure levels [25]. Figure 14 shows how the 27-sector model is sensible to these changes, while the 3-sector one returns always the same profile, independent of the width. In particular, a narrow contact induced higher wear in the centre of the tyre and a wide one in the region between the centre and the two shoulders [40], because it is in contact both at small and high roll angles.

In conclusion, the 3-sector model is able to reproduce the principal characteristic of the tyre wear profile, while increasing the number of sectors achieves a finer representation level of the wear on the tyre, making the model more sensible to changes in

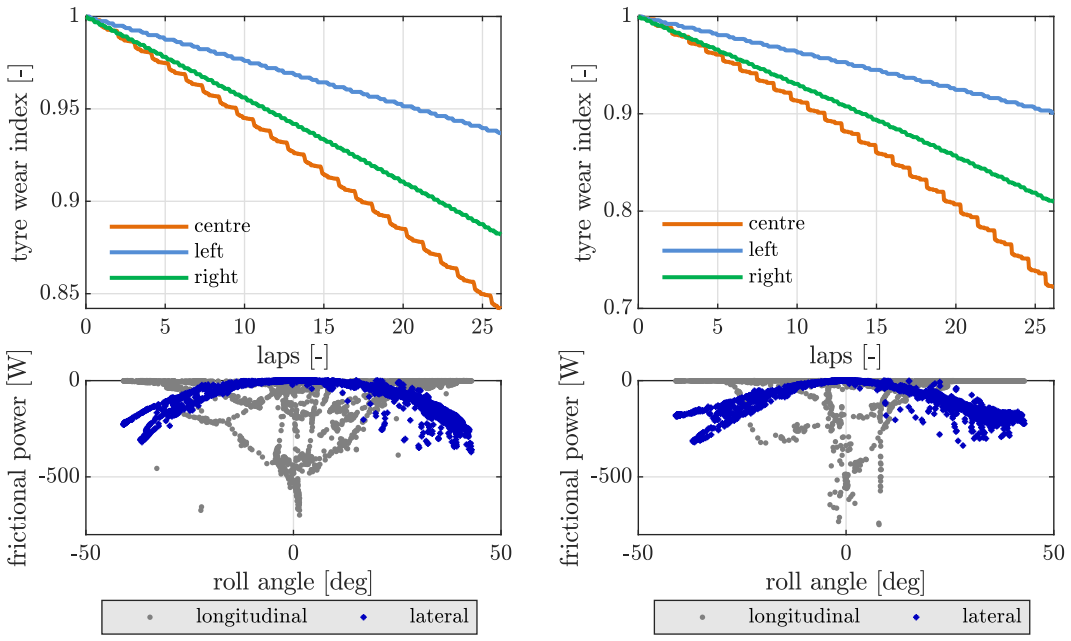

(a) Rear. (b) Front.

Figure 11.: Time evolution of the tyre wear index associated with each sector for front and rear tyre, associated to the frictional power roll distribution.

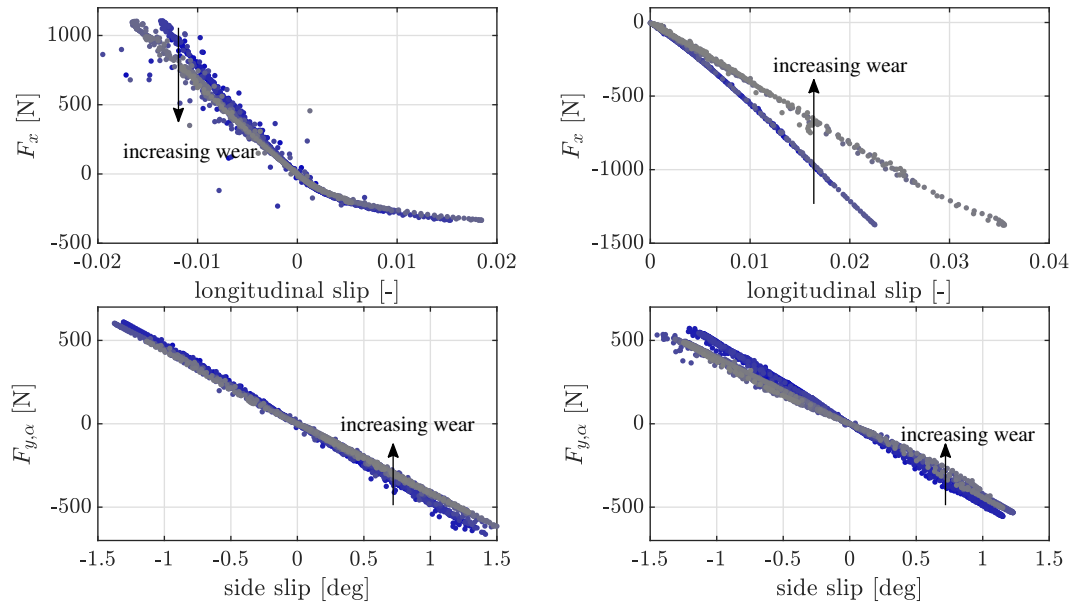

(a) Rear. (b) Front.

Figure 12.: Longitudinal (top) and lateral (bottom) frictional forces associated to the first laps (darker) and last laps (lighter).

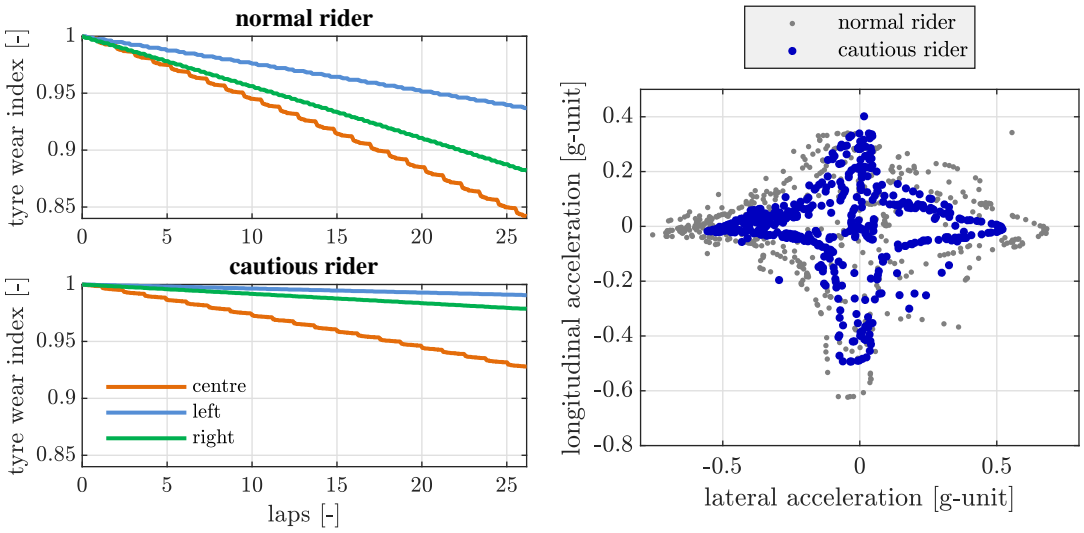

(a) Rear tyre wear indexes.

(b) gg-plot for the two different riding styles.

Figure 13.: Tyre wear index is sensible to riding style showing lower wear for a more cautious riding style.

the parameters.

6. Conclusions

A simulation-oriented model for tyre wear quantification associated with the effect on longitudinal and lateral tyre forces has been developed, exploiting the aspects needed to make it suitable for motorcycles. The proposed model advantages are the capability of producing the main effect of the tyre wear on the vehicle dynamics and its easy integration with real-time simulation environments. Another important feature of the model is its scalability, indeed second-order effects, due to pressure or temperature variations, can be included with just a few more steps. The user can also choose the number of sectors that divides the tyre profile with respect to roll angle, in order to increase the model accuracy. Moreover, no particular difficulties arise when the wear effects on the forces of a specific tyre want to be taken into account by accurately identifying the relation between the tyre wear index and the Pacejka's *magic formula* parameters.

Declaration of interest

The authors report there are no competing interests to declare.

References

[1] Baldwin JM, Bauer DR. Rubber Oxidation and Tire Aging - A Review. Rubber Chemistry and Technology. 2008 05;81(2):338–358.

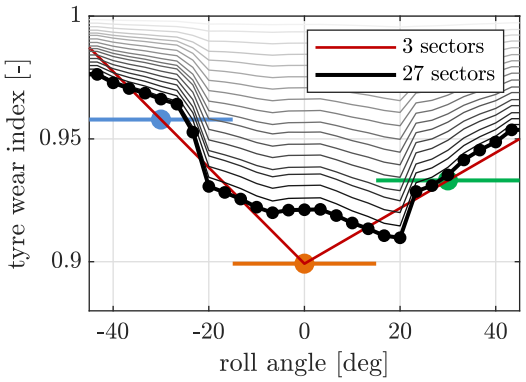

(a) Normal contact patch. The time evolution (from light to dark) of the interpolated tyre wear index is reported for the 27-sector index.

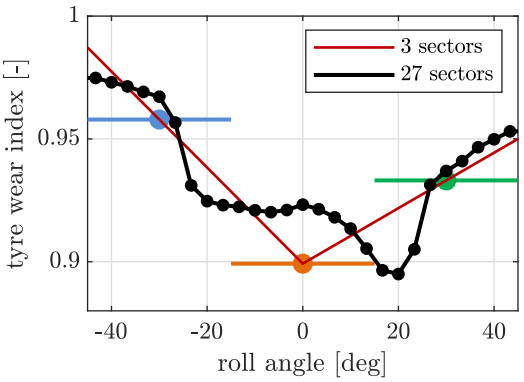

(b) Wide contact patch.

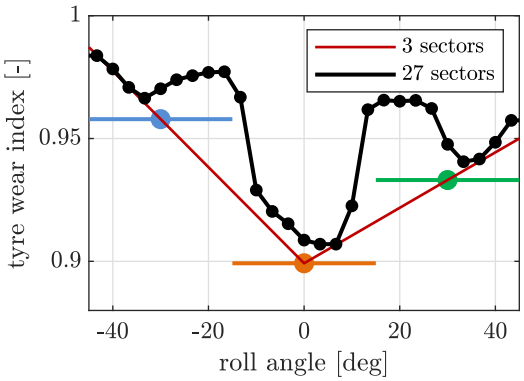

(c) Narrow contact patch.

Figure 14.: The 27-sector index compared with the 3-sector one, for different values of contact width.

[2] Grosch K. Rubber abrasion and tire wear. Rubber Chemistry and Technology. 2008; 81(3):470–505.

[3] Le Maitre O, Süssner M, Zarak C. Evaluation of tire wear performance. SAE Technical Paper; 1998.

[4] Braghin F, Cheli F, Melzi S, et al. Tyre wear model: validation and sensitivity analysis. Meccanica. 2006;41(2):143–156.

[5] Braghin F, Cheli F, Melzi S, et al. Sensitivity analysis of the tyre design parameters with respect to tyre wear using a physical tyre model. Vehicle System Dynamics. 2005; 43(sup1):102–110.

[6] Lupker H, Cheli F, Braghin F, et al. Numerical prediction of car tire wear. Tire Science and Technology. 2003;32(3):164–186.

[7] Kahms S, Wangenheim M. Experimental investigation and simulation of aircraft tire wear. Tire Science And Technology. 2020;49(1):55–74.

[8] Nguyen V, Zheng D, Schmerwitz F, et al. An advanced abrasion model for tire wear. Wear. 2018;396:75–85.

[9] Chang J, Chenyuan H, Xiaoxiong J. FE simulation of tire wear with complicated tread pattern. Procedia Engineering. 2011;15:5015–5019.

[10] Cho J, Jung B. Prediction of tread pattern wear by an explicit finite element model. Tire science and Technology. 2007;35(4):276–299.

[11] Zheng D. Prediction of tire tread wear with FEM steady state rolling contact simulation. Tire Science and Technology. 2003;31(3):189–202.
[12] D'Avico L, Tanelli M, Savaresi SM. Tire-wear control in aircraft via active braking. IEEE Transactions on Control Systems Technology. 2021;29(3):984–995.
[13] Tandy D, Pascarella R, Neal J, et al. Effect of tire wear on tire force and moment characteristics. Tire Science and Technology. 2010;38(1):47–79.
[14] Wright KRS, Botha TR, Els PS. Effects of age and wear on the stiffness and friction properties of an suv tyre. Journal of Terramechanics. 2019;84:21–30.
[15] Singh KB, Sivaramakrishnan S. An adaptive tire model for enhanced vehicle control systems. SAE International Journal of Passenger Cars-Mechanical Systems. 2015;8(2015-01-1521):128–145.
[16] Farroni F, Sakhnevych A, Timpone F. Physical modelling of tire wear for the analysis of the influence of thermal and frictional effects on vehicle performance. Proceedings of the Institution of Mechanical Engineers, Part L: Journal of Materials: Design and Applications. 2017;231(1-2):151–161.
[17] West WJ, Limebeer DJN. Optimal tyre management for a high-performance race car. Vehicle System Dynamics. 2022;60(1):1–19.
[18] Mastinu G, Gaiazzi S, Montanaro F, et al. A semi-analytical tyre model for steady-and transient-state simulations. Vehicle system dynamics. 1997;27(S1):2–21.
[19] Pacejka HB. Tire and vehicle dynamics. 3rd ed. Oxford: Butterworth-Heinemann; 2012.
[20] Pacejka HB, Besselink IJM. Magic formula tyre model with transient properties. Vehicle System Dynamics. 1997;27(sup001):234–249.
[21] Li Y, Zuo S, Lei L, et al. Analysis of impact factors of tire wear. Journal of Vibration and Control. 2012;18(6):833–840.
[22] Smith ND. Understanding parameters influencing tire modeling. Formula SAE Platform, Department of Mechanical Engineering, Colorado State University. 2004;.
[23] Pacejka HB, Bakker E. The magic formula tyre model. Vehicle System Dynamics. 1992; 21(sup001):1–18.
[24] Besselink IJ, Schmeitz AJ, Pacejka HB. An improved Magic Formula/Swift tyre model that can handle inflation pressure changes. Vehicle System Dynamics. 2010;48(sup1):337–352.
[25] Cossalter V, Doria A, Giolo E, et al. Identification of the characteristics of motorcycle and scooter tyres in the presence of large variations in inflation pressure. Vehicle System Dynamics. 2014;52(10):1333–1354.
[26] Becker C, Els S. Effect of surface roughness on tyre characteristics. Journal of Terramechanics. 2022;102:27–48.
[27] Capra D, Farroni F, Sakhnevych A, et al. On the implementation of an innovative temperature-sensitive version of pacejka's mf in vehicle dynamics simulations. In: Proceedings of XXIV AIMETA Conference 2019; 2019. p. 1084–1092.
[28] Farroni F, Giordano D, Russo M, et al. Thermo racing tyre a physical model to predict the tyre temperature distribution. Meccanica. 2014;(3):707–723.
[29] Tremlett AJ, Limebeer DJN. Optimal tyre usage for a formula one car. Vehicle System Dynamics. 2016;54(10):1448–1473.
[30] Farroni F, Mancinelli N, Timpone F. A real-time thermal model for the analysis of tire/road interaction in motorcycle applications. Applied Sciences. 2020;10(5).
[31] Kemp I. Influence of front tyre wear on wet braking performance of medium trucks. SAE Transactions. 1988;97:897–905.
[32] De Vries E, Pacejka H. Motorcycle tyre measurements and models. Vehicle System Dynamics. 1998;29(sup1):280–298.
[33] Lot R. A motorcycle tire model for dynamic simulations: Theoretical and experimental aspects. Meccanica. 2004;39(3):207–220.
[34] Cossalter V. Motorcycle dynamics. 2nd ed. Lulu.com; 2006.
[35] Blundell M, Harty D. The multibody systems approach to vehicle dynamics. 2nd ed. Oxford: Butterworth-Heinemann; 2014.

[36] Tezuka Y, Ishii H, Kiyota S. Application of the magic formula tire model to motorcycle maneuverability analysis. JSAE Review. 2001;22(3):305–310.
[37] Gelmini S, Centurioni M, Pivaro N, et al. A data-driven, vehicle-independent usage monitoring system for shared fleets: Assessing vertical and longitudinal wear. IEEE Vehicular Technology Magazine. 2022;17(1):85–93.
[38] Colombo T, Panzani G, Savaresi SM, et al. Absolute driving style estimation for ground vehicles. In: 2017 IEEE Conference on Control Technology and Applications (CCTA); 2017. p. 2196–2201.
[39] Kalabić U, Chakrabarty A, Quirynen R, et al. Learning autonomous vehicle passengers' preferred driving styles using g-g plots and haptic feedback. In: 2019 IEEE Intelligent Transportation Systems Conference (ITSC); 2019. p. 4012–4017.
[40] Andersson-Sköld Y, Johannesson M, Gustafsson M, et al. Microplastics from tyre and road wear a literature review. Swedish National Road and Transport Research Institute (VTI); 2020.